

Effect of the Nature, the Content and the Preparation Method of Zeolite-Polymer Mixtures on the Pyrolysis of Linear Low-Density Polyethylene

Paola Arango-Ponton, Guillaume Corjon, Jérémy Dhainaut, Sophie Heymans, Sophie Duquesne,* and Jean-François Lamonier*

The effect of the preparation method of the mixture catalyst/polymer on the linear low-density polyethylene (LLDPE) pyrolysis is studied by comparing the results obtained when the polymer and the catalyst (H β or HZSM-5) are extruded or simply mixed in powder form. By improving the polymer/catalyst contact through extrusion, the polymer degradation took place at lower temperature. The effect of extrusion is more pronounced with H β compared to HZSM-5 owing to the highest external surface of H β . While the yields of gas/liquid/coke do not differ with the preparation method when HZSM-5 is used as catalyst, more significant amount of liquid phase and high production of paraffins are observed when H β /LLDPE mixture is extruded, according to random scission pathway reactions. The subsequent reactions are limited by the size of the pore, which impede hydrogenation reactions, producing high molecular weight molecules. Regardless of zeolite type, the micropores of the zeolite are more affected by deactivation by coke when extrusion method is used, this effect being much more important for HZSM-5. This result is a consequence of a polymer pre-degradation during the extrusion process in which the first cracks of the polymer at low temperature and the first pore blockages can be generated.

the non-catalytic route. In recent times, the process of plastic recycling via catalytic pyrolysis has garnered heightened attention within the scientific community, as evidenced by various scientific review articles.^[4–8] It significantly reduces the pyrolysis temperature and can direct the reaction to desired liquid pyrolysis products.^[9] The main products obtained from catalytic pyrolysis of polyolefins include aromatic hydrocarbons such as benzene, toluene, ethylbenzene, and xylene (BTEX), valuable chemicals widely used in the petrochemical industry.^[10–12] For example, toluene is one of the raw materials for caprolactam or polyurethane production, and xylenes are used as solvents.^[10,13] Zeolites are the most used catalysts in the pyrolysis of plastics due to their high specific surface area and acidic properties, favoring a lower reaction temperature and promoting higher selectivity in BTEX compared to thermal cracking.^[14–26]


Different types of zeolites have been reported to efficiently affect the pyrolysis of plastics in general and of polyethylene (PE) in particular^[4] due to their catalytic activity, control of product distribution and reduction of undesirable by-products. Zeolites are solid crystalline structures described as crystalline aluminosilicate sieves that have open pores and ion exchange capacity and are obtained by means of a three-dimensional interlacing where oxygen atoms join the tetrahedral

1. Introduction

Pyrolysis is considered a promising way to tackle plastic pollution. It allows polymer decomposition under the action of temperature in the absence of oxygen and leads to the recovery of various essential chemical products.^[1–3] Considering different pyrolysis processes, catalytic pyrolysis has several benefits over

P. Arango-Ponton, J. Dhainaut, J.-F. Lamonier
CNRS
Université Lille
Centrale Lille
Univ. Artois
UMR 8181 – UCCS – Unité de Catalyse et Chimie du Solide
59000 Lille, France
E-mail: jean-francois.lamonier@univ-lille.fr

G. Corjon, S. Duquesne
CNRS
Université Lille
INRAE
Centrale Lille
UMR 8207-UMET-Unité Matériaux et Transformation
59000 Lille, France
E-mail: sophie.duquesne@centralelille.fr

 The ORCID identification number(s) for the author(s) of this article can be found under <https://doi.org/10.1002/aesr.202400072>.

© 2024 The Author(s). Advanced Energy and Sustainability Research published by Wiley-VCH GmbH. This is an open access article under the terms of the Creative Commons Attribution License, which permits use, distribution and reproduction in any medium, provided the original work is properly cited.

S. Heymans
Zone Commercial
NeoEco
1 Rue de la Source, 59320 Hallennes-lez-Haubourdin, France

DOI: 10.1002/aesr.202400072

sides. They are made of silica and alumina, and their relationship determines their reactivity, effectiveness, and acidity and affects the final product of plastic waste pyrolysis.^[4,27,28] Boronat et al.^[29] highlight the significance of the local geometry of the Al–O(H)–Si group in zeolites as a crucial factor affecting acidity. Specifically, the range of T–O–T angles plays a pivotal role in determining the acidity level of different zeolite materials. Strongly acidic zeolites like HZSM-5 and mordenite exhibit a wider range of T–O–T angles, spanning from 137° to 177° and 143° to 180°, respectively. In contrast, less acidic materials like HY demonstrate narrower T–O–T angle ranges, typically from 138° to 147°. This observation underscores the influence of local geometric variations on the acidity properties of zeolites.

The ratio of polymer to catalyst is another critical determinant of pyrolysis outcome. Studies have demonstrated that altering this ratio significantly affects gas and liquid product yields, with implications for product composition. A study by Mastral et al.^[30] investigated the cracking of high-density polyethylene (HDPE) using a nanocrystalline HZSM-5 zeolite catalyst. It was observed that at a temperature of 500 °C, the lowest gas yield during thermal cracking was obtained. Conversely, when the polymer-to-catalyst ratio decreased to 0.93, the gas yield increased significantly to 80.13%, with a high content of C₄ hydrocarbons. In contrast, in this case, the liquid phase is made up mainly of cycled and aromatics hydrocarbons, while in thermal cracking, the liquid phase is made up mainly of paraffins (C₁₀–C₂₀) and olefins. Interestingly, when the polymer-to-catalyst ratio exceeded 7, there was a sudden decrease in gas yield.

In contrast, efficient pyrolysis not only depends on the physicochemical properties and catalyst content but will also be achieved with a homogeneous contact between the polymer and the solid catalyst.^[27] The lack of homogeneity between the polymer and the catalyst in the process has led some authors to favor the use of agitation during the reaction^[31,32] to obtain a better heat transfer, a higher proportion of the liquid phase (pyrolysis oil) and greater reactivity of the catalysts.^[33] Nevertheless, using these reactors implies high operating costs and favors the deactivation of the catalyst, reasons why their use on a large scale is not recommended.^[33,34] Another option to get homogeneous contact between the catalyst and the polymer is extrusion, which has recently attracted interest.^[35] Extrusion allows excellent control of the pyrolysis residence time and efficient and better contact between the catalyst and the polymer.^[31] Marcilla et al.^[36] compared a dry powder mixture and a melt extrusion mixture between HDPE (80%) and zeolite HZSM-5 (20%) in both flash pyrolysis and slow pyrolysis. Similarly, Muhammad et al.^[37] and Caldeira et al.^[38] studied the effect of pre-degradation treatment and thermal homogenization with an extrudate in catalytic (Y zeolite) pyrolysis of LLDPE and LDPE, respectively. The pre-degradation treatment consists of heating the mixture of polymer and catalyst in powder form to 120–180 °C for 10 min,^[37] while the thermal homogenization consists of an additional step of thermal treatment at 120 °C (isotherm for 6 h) before pyrolysis. They show that both processes favored the catalytic process at lower temperatures. Serrano et al.^[39,40] used extrusion in the thermal and catalytic degradation of LDPE through a continuous process using a screw kiln reactor. They evaluated the difference between a screw kiln reactor and a batch reactor in the thermal degradation of LDPE,

obtaining a more significant amount of liquid and content in olefins when the extrusion system is used.^[39] The authors also showed that using lubricating oil at different concentrations as an additive in the extrudate can significantly improve the catalyst-polymer contact.^[40] Most recently, Martey et al.^[35] studied the effect of extrusion speed and catalyst composition and concentration on the pyrolysis of LDPE. A hybrid chemical-mechanical approach using reactive twin-screw extrusion (TSE) was used. They showed that LDPE extruded with Y zeolite shows lower degradation temperature and increased short-chain branching. Mesoporous MCM-41 also induces increased branching but does not affect the degradation temperature, possibly due to the low concentration of acid sites, which could generate a fast blockage or deactivation of active sites after extrusion.

Despite the extensive body of research dedicated to catalyst properties and preparation methods for plastic pyrolysis, a notable gap persists in the literature regarding the holistic exploration of how these factors collectively influence catalytic polymer pyrolysis outcomes. This study aims to bridge this gap by undertaking a systematic investigation into the synergistic effects of catalyst properties and preparation methods on polymer pyrolysis. In particular, our research endeavors to elucidate the comparative impact of polymer-catalyst extrusion versus an alternative preparation method, an aspect that has not received adequate attention thus far, through the use of two preselected zeolites characterized by distinct physicochemical properties, thereby enabling a nuanced analysis of how different preparation methods interact with zeolite characteristics to modulate pyrolysis products. We seek to uncover whether the observed effects are contingent upon the specific type of zeolite employed, thus offering invaluable insights into tailored pyrolysis processes. Moreover, our investigation extends beyond methodological comparison to scrutinize the influence of zeolite/polymer ratio on pyrolysis performance, a crucial aspect for optimizing pyrolysis reactions.

2. Results and Discussion

2.1. Effect of Zeolite Composition on LLDPE Pyrolysis

The first step of this study is to investigate the effect of the type of zeolite on the pyrolysis of LLDPE. **Figure 1A** shows the thermogravimetric analysis (TGA) curves obtained for the thermal pyrolysis of LLDPE and five zeolites-LLDPE mixtures with a catalyst:polymer ratio 1:1. **Figure 1B** exhibits the corresponding derivative thermogravimetry (DTG) curves. According to the literature, the thermal pyrolysis of LLDPE occurs in a single stage,^[41] which is confirmed in our study. In the presence of a catalyst, the pyrolysis of PE also occurs in one main stage. However, a shoulder toward the lowest temperatures is visible on the DTG curves (**Figure 1B**), in particular for the H β (25) catalyst. An observable initial degradation step is also evident at lower temperatures when NaY is used. This phenomenon can be ascribed to water molecules absorbed within the zeolite framework, which may have been introduced during storage or through the mixing process with the LLDPE.^[42]

Figure 1 also shows that the presence of catalysts allows a noticeable reduction in the maximal temperature of degradation, and this permits the achievement of high activity. In order to

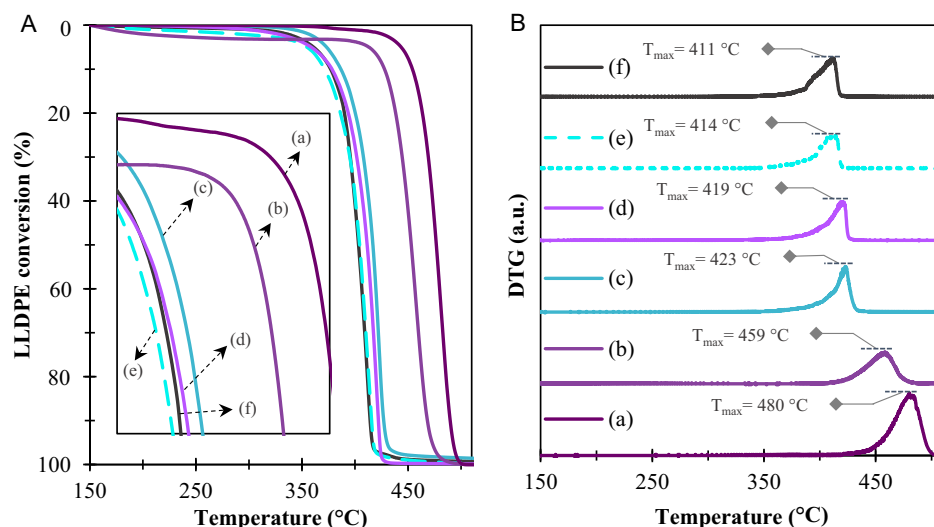


Figure 1. A) LLDPE conversion and B) DTG curves obtained when degrading pure LLDPE or mixed with a catalyst (ratio catalyst:polymer, 1:1) under nitrogen atmosphere: a) no catalyst, b) NaY (5.1), c) H β (360), d) HZSM-5 (23), e) HY (5.1), and f) H β (25).

easily discuss the effect of the catalyst on the characteristic pyrolysis temperature of LLDPE, Table S1, Supporting Information, shows the temperatures T_{max} , $T_{5\%}$ and $T_{95\%}$, as well as the relative catalytic activity of the zeolites, denoted ΔT_{max} .

Based on ΔT_{max} , the following rank can be established: H β (25) \approx HY (5.1) > HZSM-5 > H β (360) > NaY. The lowest activity of the NaY zeolite compared to the protonic form of the other studied zeolites can be explained by the difference in the acidity of the material (Table 3). Indeed, if we compare NaY and HY zeolites, which are two Y zeolite based on sodalite cage that is joined by O-bridges between the hexagonal faces (FAU structure) presenting similar Si/Al ratio (5.1), it is known that the acidity in a proton-type zeolite (HY) is higher than that of sodium-type Y zeolites (NaY). Similarly to what was found by I.C. Neves et al.^[43] a decrease in the characteristic temperature of pyrolysis ($T_{5\%}$ and $T_{95\%}$ in our study and T_{onset} in^[43]) is observed compared to PE and is higher in the case of HY. On the contrary, and as expected, H β (25) is more active compared to H β (360). The difference may be attributed to the fact that the acidity of zeolites is driven by the amount of Brønsted and Lewis acid sites formed by the replacement of Si⁴⁺ in tetrahedral position by Al³⁺ forming a Si-OH-Al group (Brønsted)^[44] and the dehydroxylation of this group (Lewis).^[12] The more aluminium atoms replacing silicon atoms (lower SiO₂/Al₂O₃ ratio), the higher the amount of Brønsted and Lewis acid sites, thus the higher the acidity.^[45,46] Agullo et al.^[47] reported comparable findings in their study. They conducted experiments by mixing LDPE with 20 wt% of zeolite H β having varying SiO₂/Al₂O₃ ratios (25, 150, and 300). At lower SiO₂/Al₂O₃ ratios, the catalytic activity increased, which was attributed to a higher concentration of Brønsted and Lewis acid sites present in the zeolite. H β (25) exhibits superior activity compared to HZSM-5 (23), as illustrated in Figure 1. According to Tian et al.^[42] the cracking of low-density polyethylene (LDPE) by H β (ratio polymer:catalyst, 2:1) occurs in two stages. The first stage occurs at lower temperatures (between 250 and 320 °C) at the catalyst surface, facilitated by greater accessibility of the

polymer to acid sites located outside the pores. This leads to more scissions occurring outside the pores. In contrast, HZSM-5 zeolite predominantly cracks LDPE within the pores in an apparent single stage (ratio polymer:catalyst, 2:1). The lower activity of HZSM-5 is attributed to its microporous structure and larger crystal size, which hinder the diffusion of long-chain molecules to the microporous acid sites.^[48]

Based on those results, it was decided to look in more detail at the performances of the H β (25) catalyst due to its highest catalytic effect by comparing it to the HZSM-5 (23) catalyst. HZSM-5 catalyst was selected as a reference since it is the most used in polymer pyrolysis.^[6,49] Moreover, both zeolites present similar SiO₂/Al₂O₃ ratios, and their specific surface and total acidity are in the same range.

2.2. Effect of the Preparation Method of the Mixture

The effect of the preparation method of the mixture catalyst/polymer on the LLDPE pyrolysis was studied by comparing the results obtained when the polymer and the catalyst (H β or HZSM-5) were extruded or simply mixed in powder form, both cases with a catalyst:polymer ratio equal to 1:10. It must be clarified that no effect of extrusion on the polymer alone has been observed, as the recorded mass losses during pyrolysis of the extruded and powdered polymer were found to be identical (not shown).

Figure 2 shows the TG and DTG curves obtained during the pyrolysis under nitrogen of a LLDPE/H β (25) and LLDPE/HZSM-5 (23) mixtures achieved by extrusion or simple powder mixture. The catalytic pyrolysis of the polymer is impacted by the mixing procedure. Indeed, when the polymer-catalyst mixture is prepared by extrusion, the degradation process occurs at lower temperatures. This improved catalytic activity could be explained by better contact between the polymer and the catalyst achieved with the extrusion. Muhammad et al.^[37] and Caldeira et al.^[38] studied the effect of pre-degradation treatment and thermal

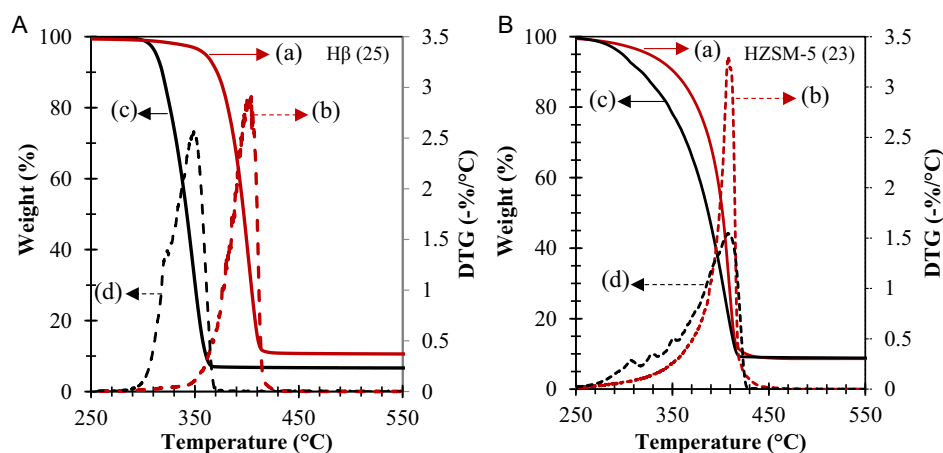


Figure 2. TGA curves a and c) and DTG curves b and d) obtained during the pyrolysis under nitrogen atmosphere of A) a LLDPE/ H β (25) and B) LLDPE/ HZSM-5 (23) mixtures achieved by simple powder mixing (red lines) or by extrusion (black lines) using a ratio catalyst:polymer 1:10.

homogenization, respectively, in the catalytic (Y zeolite) pyrolysis of polyethylene. Compared to the normal mixing, the degradation curve (TG) shifted to slightly lower temperatures with pre-degradation treatment. Using the thermal homogenization process, the degradation curve (TG) shows one mass loss, while two mass losses are clearly identified without thermal homogenization. Then, it could be suggested that normal mixing of the polymer with the catalyst allows a fraction of the polymer to be decomposed at lower temperatures by the catalytic pathway, while the non-catalytic thermal pathway degrades the remaining polymer. By improving the contact between the polymer and the catalyst through extrusion, the catalytic pathway is certainly promoted, and the polymer degradation takes place at a lower temperature.

The effect of extrusion is more pronounced when H β is employed compared to HZSM-5. As previously mentioned, this result could be explained by the external surface of the H β zeolite, which is ≈ 6 times larger than that of the HZSM-5 zeolite (Table 3). These results thus show that the effect of the preparation method could vary from one catalyst to another depending on their physicochemical properties. Since the external surface has a crucial role in the catalytic activity of zeolite in pyrolysis reaction, the preparation method will have a more critical effect when this external surface is important.

2.3. Effect of the Preparation Method of the Mixture on the Yield and Selectivity of the Pyrolysis Reaction of LLDPE

This part of the study investigated the effect of the preparation method on the yield and selectivity of the pyrolysis reaction of LLDPE. Indeed, the data obtained by TGA only gives information on the activity, i.e., pyrolysis kinetics. The pyrolysis products have been categorized by phase type (gas, wax+oil, and coke), by the family of products (paraffins, olefins, and aromatics) and according to their carbon distribution (C₃–C₅, C₆–C₁₂, and \geq C₁₃), these last two considering only the liquid phase. It should be noted that LLDPE conversion is complete at given pyrolysis conditions.

2.3.1. Catalytic Pyrolysis of LLDPE using H β (25)

Figure 3A shows the effect of the preparation method on the gas/liquid/coke yields in the LLDPE catalytic degradation in the presence of H β zeolite. The H β /LLDPE extruded mixture yields a higher amount of liquid than the powdered H β /LLDPE mixture. Zeolite H β has a large pore size with 12-ring three-dimensional channels (5.6 \times 5.6 and 6.6 \times 6.7 Å) perpendicularly intersecting.^[50] Its larger external surface (36.9% of the total surface) promotes the cracking reaction at the external surface, and its large pore size allows faster mass transfer through the channels.^[51] Considering the mechanical action of the extrusion and since the external surface of H β zeolite is high, LLDPE cracking on the external surface will be favored, which could explain the more significant amount of liquid phase when the extruded material is used. The coke yields were very low (<1%) and were similar regardless of the preparation method used.

The wax+oil fraction is mainly composed of i-olefins and i-paraffins (Figure 3B). The small selectivity of aromatic compounds obtained in this part of the study is also reported by other authors.^[52] In contrast, the production of i-paraffins is higher with the H β /LLDPE extruded mixture (35.4%) than with the powdered H β /LLDPE mixture (24.1%) whereas the production of n-olefin and aromatic is lower. The high production of paraffins and the low production of aromatics found after pyrolysis of the H β /LLDPE extruded mixture demonstrate a tendency toward the random scission pathway reactions^[52] when the material is extruded.

A view of the carbon distribution (Table 1) of the wax+oil products shows that the amount of C₃–C₅ range is higher for the powdered H β /LLDPE mixture than for the H β /LLDPE extruded mixture. It means that the powdered mixture promotes the LLDPE cracking into the micropores, which is in line with the amount of gas produced that is higher. The extruded and powdered mixtures have high hydrocarbon selectivity from C₆ to C₁₂, especially the extruded mixture, in this zone are located the majority of monoaromatics. Indeed, the production of BTEX with zeolite H β is between 23% and 62% of the total

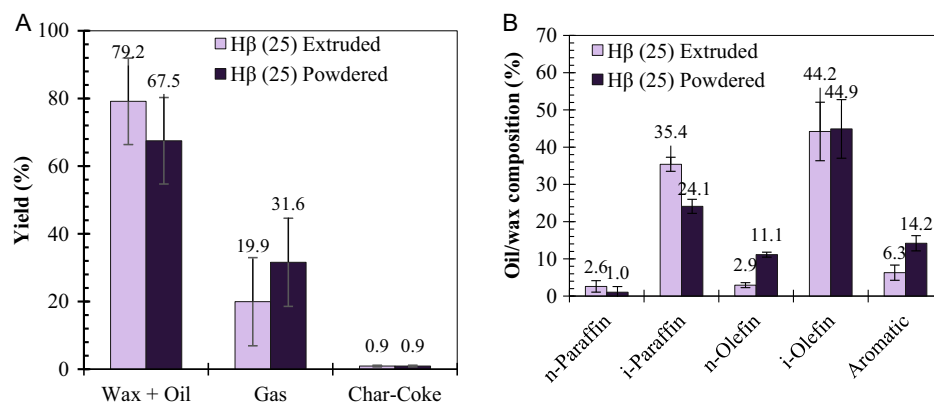


Figure 3. A) Yield result of pyrolysis of LLDPE with Hβ (25) and B) composition of oil/wax from the decomposition of LLDPE with Hβ (25) using powdered polymer (Powdered) or catalyst extruded with polymer (Extruded).

Table 1. Carbon distribution by family of products from pyrolysis of LLDPE with Hβ (25) using powdered polymer (powdered) or catalyst extruded with polymer (extruded).

Catalyst	Carbon distribution range peak area [%]		
	C ₃ –C ₅	C ₆ –C ₁₂	≥C ₁₃
Hβ (25) Extruded	10.1 ± 0.1	84.8 ± 0.4	2.8 ± 0.3
Hβ (25) Powdered	18.0 ± 0.1	77.7 ± 0.4	1.5 ± 0.3
HZSM-5 (23) Extruded	4.6 ± 1.9	91.7 ± 1.9	0.6 ± 0.3
HZSM-5 (23) Powdered	3.8 ± 1.9	93.4 ± 1.9	0.9 ± 0.2

aromatics. However, although the extruded mixture has a more extensive amount of hydrocarbons in this zone, the powdered mixture promotes a greater production of aromatics. Production of hydrocarbons with a carbon number $\geq C_{13}$ is favoured with the extruded mixture. It may result from recombination reactions of higher molecular weight carbocations that did not enter the micropores due to limitations, which corroborates the inclination for random scission pathway reactions of this mixture.

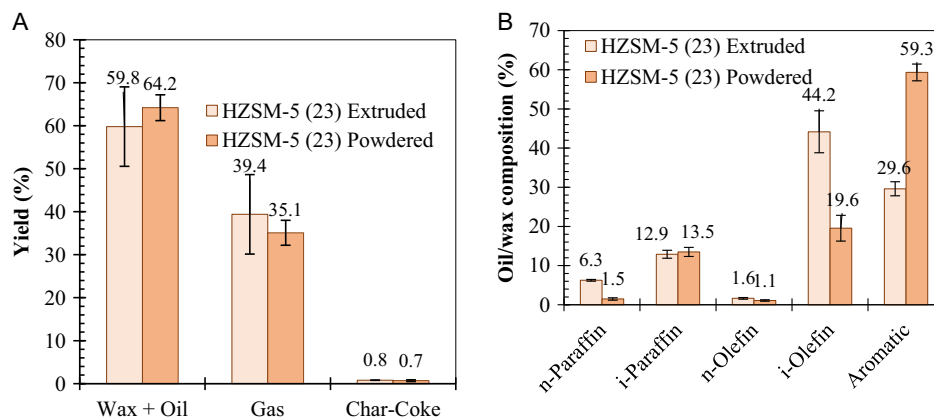


Figure 4. Yield result of pyrolysis of LLDPE with HZSM-5 (23) A) and composition of oil/wax B) from the decomposition of LLDPE with HZSM-5 (23) using powdered polymer (Powdered) or catalyst extruded with polymer (Extruded).

size^[42] and the strong Brønsted acid sites.^[12,16] The latest promotes cracking and subsequent aromatisation.^[12]

Figure 4B also shows that i-olefins are the primary products obtained when the zeolite is extruded with the polymer, whereas aromatics are favored when the catalyst is mixed as a powder with the polymer. This behavior indicates that when the LLDPE is cracking, the extruded mixture favors random scission pathways, but subsequent reactions are limited by the size of the pore, which impedes hydrogenation reactions, producing high molecular weight molecules. Indeed, Zeolite HZSM-5 has a channel system of 10 rings interconnected, with two types of channels: straight and sinusoidal. The pore sizes of these channels are 5.6×5.6 and 5.1×5.5 Å.^[50] Bimolecular reactions such as condensation or hydrogen transfer are sterically limited to form molecules of a higher molecular weight inside zeolite HZSM-5.^[41,58,59] The chain-end scission is the main reaction pathway for this zeolite due to its high acid strength, which means a more significant amount of light hydrocarbons (especially in the gas phase^[42]) and aromatics are produced.^[60]

In contrast, when the zeolite is mixed with the polymer in powder form, fewer i-olefins are produced, and more aromatics are obtained to the detriment of n-olefins production through chain-end scission pathways,^[7,61] as explained above in the description of the LLDPE reaction mechanism. The olefin aromatization is generated after LLDPE cracking through the Diels–Alder reaction.^[54]

More information on wax+oil carbon distribution is listed in Table 1. The light hydrocarbon zone (C₃–C₅) found a low production for both mixtures, especially for the powdered mixture, 3.8% compared to 4.6% of the extruded mixture. On the range of C₆–C₁₂, HZSM-5 zeolite is favourably selective in more than 90%. In both cases, in this range, the composition of the liquid phase is mainly aromatics and i-olefins. The powder mixture generated 29.7% more selectivity in aromatics, and when the extruded mixture was used, resulted in a higher selectivity of i-olefins (+24.6%), showing the preference for random scission over chain-end scission pathway reactions from the pyrolysis with the extruded mixture, which may be limited by less

accessibility to the acid sites. The carbon distribution of products with a carbon quantity greater than thirteen (>C₁₃) is insignificant for both cases, less than 1%.

2.3.3. Characterisation of the Catalyst after Pyrolysis

It was shown that depending on the catalyst type, the preparation method may affect the pyrolysis differently. It is thus also interesting to characterize the catalyst after the pyrolysis to see if the preparation method may affect the coking differently by comparing H β and HZSM-5.

The quantity of coke in the zeolites H β and HZSM-5 after the reaction has been estimated from TG analyses (Figure 5). The weight loss between 50 and 350 °C can be attributed to water removal, while the weight loss between 350 and 700 °C is ascribed to coke oxidation. Beyond 700 °C, the dealumination of the zeolite can occur.^[62] Based on the literature data, two kinds of coke can be distinguished. At low temperatures, well-structured coke species (soft coke) are oxidized, while at higher temperatures, polyaromatic coke species (hard coke) are burned.^[63,64] The quantity of soft coke is similar for the two spent HZSM-5 catalysts but not for the two spent H β catalysts, where the difference is slight but clear, while more hard coke species are present when the zeolite is extruded initially with the polymer, independent of the zeolite. The pore system of HZSM-5 imposes more significant restrictions on condensation reactions, leading to reduced coke formation compared to H β zeolite.^[58]

Figure 6 shows the XRD patterns of the fresh and spent H β (a) and HZSM-5 (b) samples. For the six zeolites, diffraction peaks for Bragg's angle between 5° and 55° can be observed and are characteristics of the tetragonal phase of the β zeolites framework (PDF-00-056-0467) for the H β samples (Figure 6A) and of the orthorhombic phase of the ZSM-5 zeolites framework (PDF-04-017-8707) for the HZSM-5 samples (Figure 6B). The two pairs of diffraction peaks of the HZSM-5 zeolites corresponding to the (3 3 2) and (0 5 1), and (8 0 4) and (0 1 0 0) lattice planes merged into a single peak at 2θ values of 23.2° and 45.1°, for the spent HZSM-5 zeolites, while for spent H β samples, a

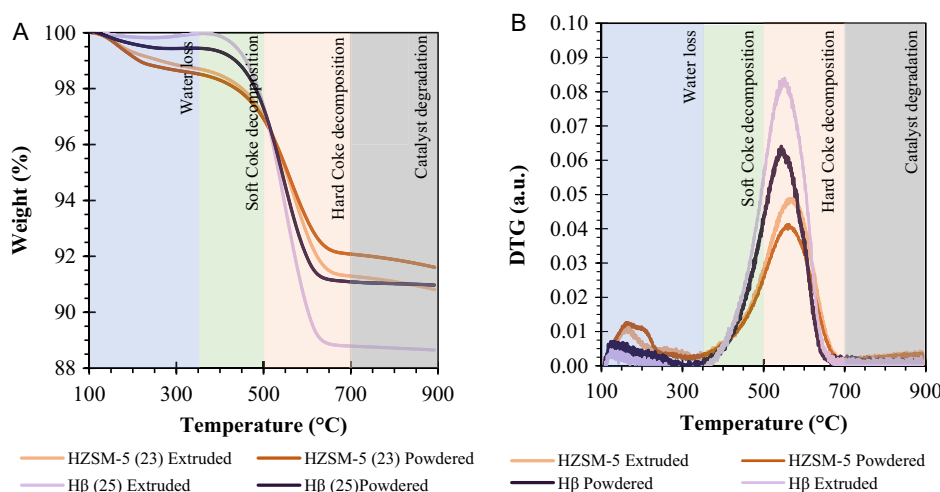


Figure 5. A) TG and B) DTG curves of H β (25) and HZSM-5 (23) zeolites after reaction using powdered catalyst-polymer mixture (Powdered) or catalyst extruded with polymer (Extruded) under air.

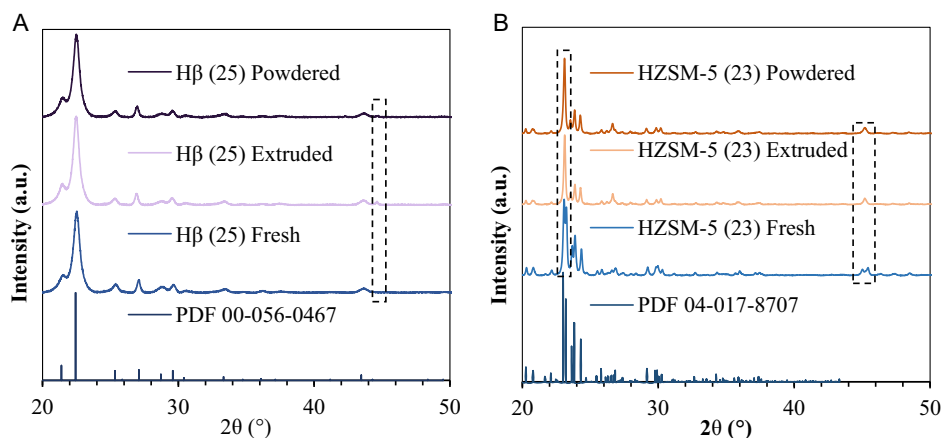


Figure 6. A) XRD of H β (25) and B) HZSM-5 (23) zeolites before reaction (Fresh) and after reaction using powdered catalyst-polymer mixture (Powdered) or catalyst extruded with polymer (Extruded).

single peak at 2θ value of 44.6° appears. After testing, this change in the crystallinity can be correlated with coke formation within the pores.^[65]

The N_2 -physisorption curves (not shown) obtained for the fresh and spent H β and HZSM-5 samples are type IV, with pronounced H4 hysteresis loops at P/P_0 greater than 0.4, according to the IUPAC nomenclature^[66] and are generally observed with materials containing both micropores and mesopores.^[67] The main textural data extracted from these curves are given in Table 2.

After the pyrolysis reactions, a significant decrease in the textural properties is observed. This decrease could be related to the coke formation in the zeolite, which blocks the pores.^[53] Deactivation by coke can be generated directly in two ways: into the micropores, where only these are deactivated, or at the external surface, where the entrance to the micropores is blocked and therefore deactivated. H β (25) external surface is affected in equal proportion for the extruded and powdered mixture. Due to the large size of the pores of zeolite H β , it is easier to block the micropores than the pore entrances because its large pore size allows greater diffusion of by-products into the inside of the zeolite. It has been reported that the coke in zeolite H β prefers to be located near strong acid sites, in the ultramicropores of the structure or blocking its access.^[68] Hence, the external surface is less affected.

Table 2. Textural properties of H β (25) and HZSM-5 (23) zeolites before reaction (fresh) and after reaction using powdered catalyst-polymer mixture (powdered) or catalyst extruded with polymer (extruded).

Catalyst	S_{BET} [$\text{m}^2 \text{g}^{-1}$]	S_{EXT} [$\text{m}^2 \text{g}^{-1}$]	S_{MICRO} [$\text{m}^2 \text{g}^{-1}$]
HZSM-5 (23) Fresh	413	30	383
H β (25) Fresh	523	193	330
HZSM-5 (23) Extruded	90 (−78%)	10 (−67%)	80 (−79%)
HZSM-5 (23) Powdered	178 (−57%)	14 (−53%)	165 (−57%)
H β (25) Extruded	287 (−45%)	156 (−19%)	132 (−60%)
H β (25) Powdered	330 (−37%)	155 (−20%)	175 (−47%)

Indistinctively from zeolite, the micropores are more affected by deactivation by coke when extrusion is used, this effect being much more important for zeolite HZSM-5. This behaviour can be explained as a consequence of a polymer pre-degradation during the extrusion process in which the first cracks of the polymer at low temperature and the first pore blockages can be generated.

In the case of zeolite HZSM-5, the deactivation is more intense, possibly due to its pore size. In the powdered test, there is a higher coke formation on the surface because the deactivation is in the same proportion both on the external surface and in the micropores. The deactivation can be explained by considering that coke deposition on the external surface blocks access to the micropores and, therefore, the internal acid sites.^[69] In other words, the smaller size of the pores enables a relatively straightforward obstruction of their entrances, concurrently deactivating all active sites within the pores. On the contrary, the extrusion method allows the diffusion of products in the micropores, where these products are exposed to more acid sites and an over-cracking, forming mainly polyaromatics (hard coke);^[65] in other words, there is an important migration of coke in the micropores which could restrict the aromatization reaction of the olefins.

2.4. Effect of the Ratio Catalyst/Polymer on the Yield and Selectivity of the Pyrolysis Reaction of LLDPE

It is also essential to emphasize that the extrusion process offers distinct advantages over existing literature. We can operate within a broader range of concentrations by employing extrusion, enabling greater flexibility in the experimental conditions. Moreover, the extrusion method allows for improved homogeneity control. This enhanced control over concentration and homogeneity enhances the reliability and accuracy of our experimental findings.

In order to be able to vary the catalyst:polymer ratio in a wide range and to study the effect of a small amount of catalyst, we proceeded with the extrusion method to prepare the mixtures, which allows the control at a very low catalyst:polymer ratio. The study was conducted on two catalysts, H β (25) and HZSM-5 (23).

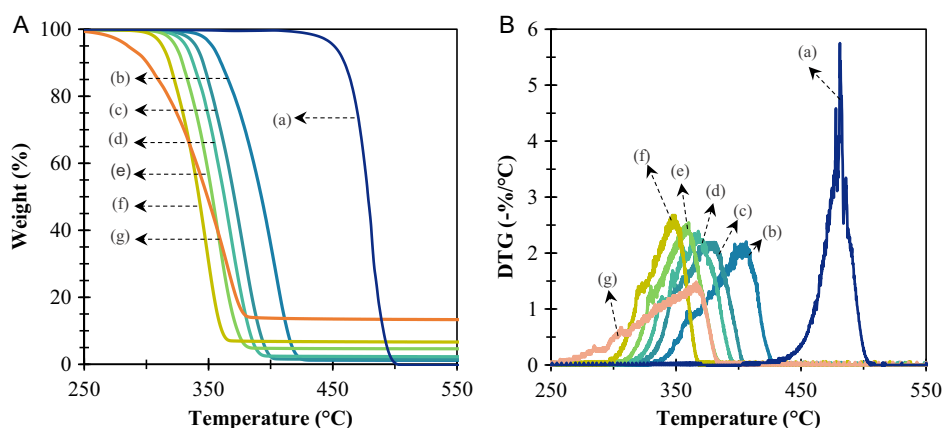


Figure 7. TG A) and DTG B) curves obtained during the pyrolysis of LLDPE under nitrogen atmosphere at $10^{\circ}\text{C min}^{-1}$ with H β (25) zeolite using different catalyst: polymer ratios: a) 0:100, b) 1:100, c) 1:50, d) 1:30, e) 1:20, f) 1:10, g) 1:5.

Figure 7A and B The TG and DTG curves, respectively, obtained during the pyrolysis of pure LLDPE or in the presence of H β (25) zeolite at various ratios. Six different catalyst:polymer ratios have been investigated from 1:100 to 1:5. **Figure 8A and B** show the TG and DTG obtained for HZSM-5 (23) zeolite. In that case, three catalyst:polymer ratios have been investigated: 1:100, 1:50, and 1:10. The primary characteristic data are listed in Table S2, Supporting Information.

The relative activity (ΔT_{max}) is lower than 100°C for all concentrations of HZSM-5 (23), making this zeolite less active than H β (25). For the optimum value of the catalyst:polymer ratio (1:10), a T_{max} difference of 55°C is recorded in favour of H β (25), 132.6°C compared to 77.3°C for H β (25) and HZSM-5 (23), respectively. The shoulder in the principal peak at lower temperatures shown in Figure 7B and 8B evidence two cracking steps, which are much less marked in the presence of HZSM-5 (23) and non-extruded conditions compared with the literature.^[23]

The lowest external surface of HZSM-5 compared to H β (in proportions of ≈ 6 times lower)^[70–72] could explain this discrepancy. It must be pointed out that the $T_{5\%}$ values obtained in the presence of HZSM-5 (23) at catalyst:polymer ratio 1:100 is $\approx 27^{\circ}\text{C}$ more compared to H β (25) at the same ratio, but the

difference decreases with the increasing catalyst concentration, at 1:50 ratio this difference is $\approx 9^{\circ}\text{C}$ and at 1:10 ratio is $\approx 3^{\circ}\text{C}$, while $T_{95\%}$ values are much higher, more than 47°C (Table S2, Supporting Information). This suggests that HZSM-5 can initiate pyrolysis of LLDPE at a relatively low temperature despite its smaller external surface area.

As shown more clearly in Figure 8, the maximum degradation temperature decreases when the amount of HZSM-5 increases. Nevertheless, the zeolites H β (25) seem to reach a possible saturation point (**Figure 9A**), which means that this increase in the amount of zeolite will reach a point where an additional quantity of catalyst has no additional effect or has a negative effect on the activity. The saturation point is found at catalyst: polymer ratio 1:10.

Marcilla et al.^[23] did a similar study with a powdered mixture. Compared to our study, they did not observe a saturation point but a continuous increase in ΔT_{max} with catalyst concentration increase. Moreover, it must be pointed out that the preparation of the H β (25):polymer mixture by extrusion led to higher ΔT_{max} values in comparison values obtained by Marcilla et al.^[23] with a powdered mixture. Such an effect is much less pronounced when HZSM-5 (23) is used as the catalyst.

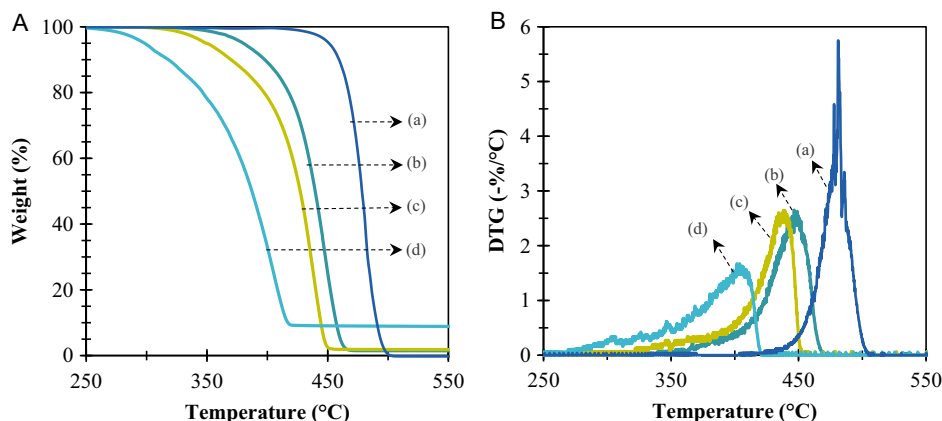


Figure 8. A) TG and B) DTG curves obtained during the pyrolysis of LLDPE under nitrogen atmosphere at $10^{\circ}\text{C min}^{-1}$ with HZSM-5 (23) zeolite using different catalyst: polymer ratios: a) 0:100, b) 1:100, c) 1:50, d) 1:10.

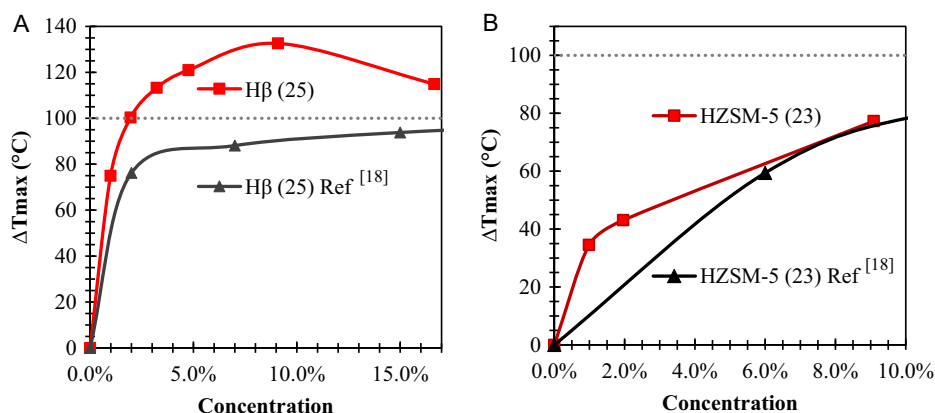


Figure 9. Comparison of the effect of the concentration of catalyst on the decomposition of LLDPE in the presence of A) Hβ (25) and B) HZSM-5 (23) zeolites on relative activity from the TG curves obtained in this study (red) and in ref.[23] (black) at 10 °C min⁻¹ under nitrogen atmosphere.

This difference in behaviour between both zeolites can be explained by the difference in external surface area, which is ≈6 times higher for Hβ (25) in comparison with HZSM-5 (23), suggesting that the mechanical effect of extrusion is experienced if the external surface of the zeolite is sufficiently high (193 m² g⁻¹).

3. Conclusions

In this study, we observed that the extrusion method for preparing zeolite-polymer mixtures has several noteworthy effects. It promotes random scission reactions, resulting in a notable increase in paraffin (17% for Hβ (25) and 4.2% for HZSM-5 (23)) and a significant increase of 25.1% in olefin production for HZSM-5 (23) zeolite. In contrast, it leads to a reduction in aromatic compound formation in the liquid phase by 7.7% and 29.7% for Hβ (25) and HZSM-5 (23), respectively. Furthermore, this method enhances the diffusion of products into micropores, resulting in more pronounced over-cracking and the formation of hard coke. Consequently, it deactivates a larger portion of the microporous surface compared to the powdered mixture method.

When comparing catalytic pyrolysis results, it is evident that the choice of zeolite significantly influences the impact of extrusion mixture cracking. Hβ zeolite, known for its extensive external surface (6 times that of HZSM-5) and larger pore size, yields 19.4% and 3.3% more liquid when subjected to extrusion and powdered mixture, respectively. In contrast, HZSM-5 (23) zeolite, with its strong Brønsted acid sites and smaller pore size, exhibits higher selectivity for aromatic compound production. Extrusion has a limited effect on liquid/gas/solid yields or soft coke production for HZSM-5 (23). However, it adversely affects the external surface and the microporous structure and leads to increased C₃–C₅ hydrocarbon production in the liquid phase.

The extrusion method was employed to reduce catalyst content, involving variations in zeolite Hβ (25) and HZSM-5 (23) concentrations within the extruded polymer. TGA revealed a two-step cracking process for Hβ (25), indicating an optimal 1:10 catalyst:polymer ratio. While HZSM-5 completes

degradation at higher temperatures ($T_{95\%} = 427.2$ °C compared to $T_{95\%}$ of Hβ (25) = 359.7 °C), the initial degradation temperature, $T_{5\%}$ equal to 315 °C, suggests it achieves decomposition at low temperatures, similar to Hβ (25) ($T_{5\%} = 312.4$ °C), within the optimal catalyst:polymer ratio of 1:10.

4. Experimental Section

LLDPE, EltexPF6220AE, provided by Wipak (Bousbecque, France), has been used in these experiments. LLDPE is in pellet form and has an average particle size of 4 mm and a density of 919 kg m⁻³. The pelleted polymer has been milled in a Retsch ZM200 ultracentrifugal mill (speed 8000 rpm) to obtain a powdered material size of 0.5 mm. Five commercial zeolites have been tested in the pyrolysis of LLDPE under nitrogen atmosphere. Before testing, all catalysts were calcinated at 600 °C for 24 h in a muffle furnace, except for HZSM-5 samples, which were calcined in flowing air (100 mL min⁻¹) according to the following protocol: ramp of 2 °C min⁻¹ from 25 to 200 °C and hold for 2 h, then a ramp of 0.5 °C min⁻¹ from 200 to 550 °C and hold for 8 h. **Table 3** shows the main characteristics of the commercial catalysts (reference, supplier, composition, and specific surface area given by the supplier).

In order to evaluate the influence of the catalyst:polymer mixtures in the catalytic pyrolysis of LLDPE, two experimental approaches have been considered. In the first one, the catalyst:polymer ratio was obtained by manually mixing the two powders. The powder LLDPE was obtained from the pelleted polymer ground in a Retsch ZM200 ultracentrifugal mill (speed 8000 rpm) to obtain a powdered material size of 0.5 mm. In the following, the suffix “powdered” is mentioned. In the second approach, the pelleted polymer and the powdered catalyst were extruded in a microextruder DSM Research 15 twin-screw model. The quantity of polymer was 10 g, and the

Table 3. Main characteristics of the catalysts used in the study.

Sample	Supplier	SiO ₂ /Al ₂ O ₃	S _{BET} [m ² g ⁻¹]	Total acidity [mmol NH ₃ g ⁻¹]
Hβ (25)	Alfa Aesar	25	523	1.48 ^[74]
HY (5.1)	Alfa Aesar	5.1	900	0.61–1.33 ^[75,76]
HZSM-5 (23)	Zeolyst	23	413	1.40 ^[74]
Hβ (360)	Alfa Aesar	360	620	0.118 ^[44]
NaY (5.1)	Alfa Aesar	5.1	900	0.40 ^[76]
Hβ (25)	Alfa Aesar	25	523	1.48 ^[74]

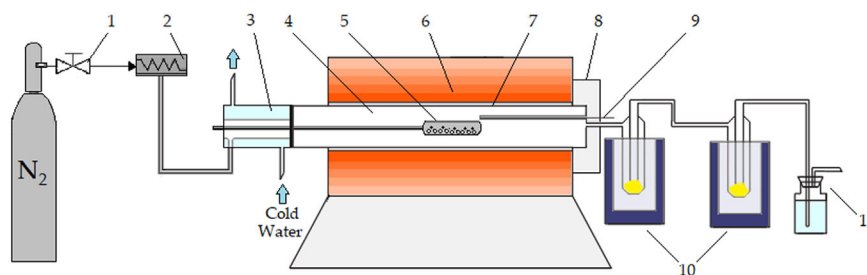


Figure 10. Schematic representation of the pyrolysis facility; 1) Gas valve; 2) Flowmeter; 3) Cold room; 4) Stainless steel tube; 5) Spoon; 6) Electric heater; 7) Heating zone; 8) Hot Chamber; 9) Thermocouple; 10) Cold traps; 11) Water-sealed bottle.

quantity of catalyst was adjusted according to the targeted catalyst:polymer ratio. The microextruder was heated at 190 °C in order to melt the polymer, then the part of the polymer was introduced and mixed for about 5 min, and the catalyst and the other part of the polymer were introduced and mixed for about 10 min. The mixing speed used was 50 rpm. At the exit of the extruder, a rod of 3 mm in diameter was obtained. In the following, the suffix “extruded” is mentioned.

The catalytic activity of the zeolites samples in the catalytic pyrolysis of LLDPE has been investigated using thermogravimetric analysis (TGA); for that purpose, the LLDPE and the catalyst were used as powder and in a 1:10 catalyst:polymer ratio. The apparatus used is a Thermal Analysis instrument (TA Q600). Pure LLDPE and a mixture of polymer and catalyst of 15 mg were pyrolysed under pure nitrogen with a flow rate of 100 mL min⁻¹. The temperature was raised from 150 to 600 °C with a heating rate of 10 °C min⁻¹. The principal parameters obtained from the TG analysis are $T_{5\%}$ and $T_{95\%}$, which represent the temperature when 5% and 95% of the LLDPE is pyrolysed, T_{max} , which is the maximal temperature of degradation of LLDPE and ΔT_{max} , which is the relative catalytic activity of the zeolite, estimated by the difference between the maximum decomposition temperature achieved by the pure polymer and the polymer-zeolite mixture. In order to evaluate the residue (coke-char) mass, the weight loss of 15 mg of catalyst + coke mixture obtained at the end of the pyrolysis process was recorded under air at a flow rate of 100 mL min⁻¹, and a heating rate of 10 °C min⁻¹ from 50 to 900 °C using the same TA Q600; the mass loss was considered to be the quantity of coke was determined between 350 and 700 °C.^[58]

The catalytic experiments were performed in a homemade stainless-steel tubular reactor heated by a furnace (CARBOLITE CERGO 30–3000 °C). For the experiments, a mixture of 1.1 g of LLPPE and catalyst (in powder form or as a pellet) was placed in a spoon justly placed in a cold room before the reaction; as described in **Figure 10**, the temperature in this room was controlled at 20 °C thanks to a chiller (LAUDA ECO SILVER). The reactor was heated at 450 °C and purged at 1 L min⁻¹ under nitrogen for 6 min. During the experiment, the gas flow was fixed at 200 mL min⁻¹. After that time, the sample was introduced to the heated zone, and the time of the experiment was fixed at 40 min. The wax+oil fraction was condensed in two cold traps immersed in liquid nitrogen. The liquid phase mass was determined by weight difference in the cold traps before and after the reaction. The gas fraction was determined through an overall mass balance of the experiment. The wax + oil, coke and gas phase yield were determined with the Equation (1–4) respectively

$$\text{Wax + oil yield (wt.\%)} = \frac{\text{Mass (Wax + Oil)}}{\text{Mass of LLDPE}} \times 100 \quad (1)$$

$$\text{Coke yield (wt.\%)} = \frac{\text{Mass Coke}}{\text{Mass of LLDPE}} \times 100 \quad (2)$$

$$\text{Gas yield (wt.\%)} = \frac{\text{Mass of LLDPE} - \text{Mass (Wax + Oil)} - \text{Mass Coke}}{\text{Mass of LLDPE}} \times 100 \quad (3)$$

$$\text{Yield} = \bar{x} \pm t_{\frac{\alpha}{2}} \left(\frac{s}{\sqrt{n}} \right) \quad (4)$$

Where \bar{x} is the average yield value, α is equal to 1 minus the confidence interval, $t_{\frac{\alpha}{2}}$ distribution is found from the t distribution table with the α value and the degrees of freedom, s is the standard deviation, and n is the number of runs. The values of the respective standard errors were calculated based on the average yields of 3 to 5 runs, with a 95% confidence interval. The standard deviation and the standard errors were obtained for each averaged yield.^[73]

The wax+oil fraction was analysed with GC-MS gas chromatography (Shimadzu GC-2010 coupled to a Shimadzu GC-MS-QP2010 Plus mass spectrometer). The GC column is a 30 m * 0.25 µm * 0.25 µm optima-5 ms capillary column. The different family yields were calculated considering only the peak area.

N₂-physisorption measurements were performed on a Micromeritics TriStarII 3020. The specific surface area was determined on ≈200 mg of powder sample previously outgassed at 150 °C under vacuum (<0.1 mbar) during a minimum of 12 h in the outgassing station. Brunauer–Emmett–Teller theory (BET) was applied to calculate the specific surface areas. Pore size distributions were obtained simultaneously from the isotherms based on the Barret–Joyner–Halenda (BJH) theory.

The powder X-Ray diffraction patterns of the samples were obtained on a Bruker AXS D8 Advance diffractometer in Bragg–Brentano geometry, Cu Kα source ($\lambda = 0.154$ nm), which was used as the radiation. The XRD pattern was recorded with a step size of 0.01° in 2θ, 1 s per step, and the range of scan was 5° < 2θ < 55°.

Supporting Information

Supporting Information is available from the Wiley Online Library or from the author.

Acknowledgements

The Chevreul Institute is thanked for its help in the development of this work through the ARCHI-CM project supported by the “Ministère de l’Enseignement Supérieur de la Recherche et de l’Innovation”, the region “Hauts-de-France”, the ERDF program of the European Union and the “Métropole Européenne de Lille”, “Initiative Science – Innovation – Territoires Economie, Université Lille Nord-Europe.”, I-Site UNLE and Neo-Eco company. The authors thank Olivier Gardoll and Laurence Burylo for their contribution to TG and XRD measurements.

Conflict of Interest

The authors declare no conflict of interest

Data Availability Statement

The data that support the findings of this study are available from the corresponding author upon reasonable request.

Keywords

catalysis, extrusion, plastic waste, polyethylene, pyrolysis, zeolite

Received: March 1, 2024

Revised: May 27, 2024

Published online:

- [1] I. Vollmer, M. J. F. F. Jenks, M. C. P. P. Roelands, R. J. White, T. van Harmelen, P. de Wild, G. P. van der Laan, F. Meirer, J. T. F. F. Keurentjes, B. M. Weckhuysen, *Angew. Chem., Int. Ed.* **2020**, 59, 15402.
- [2] A. Oasmaa, M. S. Qureshi, H. Pihkola, I. Deviatkin, J. Mannila, A. Tenhunen, H. Minkinen, M. Pohjakallio, J. Laine-Ylijoki, *J. Anal. Appl. Pyrolysis* **2020**, 152, 104804.
- [3] E. T. Aisien, I. C. Otuya, F. A. Aisien, *Environ. Technol. Innov.* **2021**, 22, 101455.
- [4] P. Kasar, D. K. Sharma, M. Ahmaruzzaman, *J. Clean. Prod.* **2020**, 265, 121639.
- [5] P. T. Williams, *Waste Biomass Valorization* **2020**, 12, 1.
- [6] Y. Peng, Y. Wang, L. Ke, L. Dai, Q. Wu, K. Cobb, Y. Zeng, R. Zou, Y. Liu, R. Ruan, *Energy Convers. Manage.* **2022**, 254, 115243.
- [7] S. Kartik, H. K. Balsora, M. Sharma, A. Saptoro, R. K. Jain, J. B. Joshi, A. Sharma, *Therm. Sci. Eng. Prog.* **2022**, 32, 101316.
- [8] M. S. Abbas-Abadi, Y. Ureel, A. Eschenbacher, F. H. Vermeire, R. J. Varghese, J. Oenema, G. D. Stefanidis, K. M. Van Geem, *Prog. Energy Combust. Sci.* **2023**, 96, 101046.
- [9] A. G. Buekens, H. Huang, *Resour. Conserv. Recycl.* **1998**, 23, 163.
- [10] G. Gałko, M. Rejdak, D. Tercki, M. Bogacka, M. Sajdak, *J. Anal. Appl. Pyrolysis* **2021**, 154, 105017.
- [11] S. B. Lee, J. Lee, Y. F. Tsang, Y.-M. M. Kim, J. Jae, S.-C. C. Jung, Y.-K. K. Park, *Environ. Pollut.* **2021**, 283, 117060.
- [12] A. A. Inayat, A. A. Inayat, W. Schwieger, B. Sokolova, P. Lestinsky, *Fuel* **2022**, 314, 123071.
- [13] J. Wang, J. Jiang, X. Meng, M. Li, X. Wang, S. Pang, K. Wang, Y. Sun, Z. Zhong, R. Ruan, A. J. Ragauskas, *Environ. Sci. Technol.* **2020**, 54, 8390.
- [14] K. Takuma, Y. Uemichi, A. Ayame, *Appl. Catal., A* **2000**, 192, 273.
- [15] R. Bagri, P. T. Williams, *J. Anal. Appl. Pyrolysis* **2002**, 63, 29.
- [16] J. Aguado, D. P. Serrano, G. San Miguel, *J. Polym. Environ.* **2007**, 15, 107.
- [17] Y. H. Lin, M. H. Yang, T. F. Yeh, M. D. Ger, *Polym. Degrad. Stab.* **2004**, 86, 121.
- [18] D. P. Serrano, J. Aguado, J. M. Rodríguez, A. Peral, *J. Anal. Appl. Pyrolysis* **2007**, 79, 456.
- [19] Y. Xue, P. Johnston, X. Bai, *Energy Convers. Manage.* **2017**, 142, 441.
- [20] K. Akubo, M. A. Nahil, P. T. Williams, *J. Energy Inst.* **2019**, 92, 195.
- [21] K. Ding, S. Liu, Y. Huang, S. Liu, N. Zhou, P. Peng, Y. Wang, P. Chen, R. Ruan, *Energy Convers. Manage.* **2019**, 196, 1316.
- [22] M. S. Renzini, U. Sedran, L. B. Pierella, *J. Anal. Appl. Pyrolysis* **2009**, 86, 215.
- [23] A. Marcilla, A. Gómez, F. Valdés, *Polym. Degrad. Stab.* **2007**, 92, 197.
- [24] J. Aguado, D. P. Serrano, J. M. Escola, E. Garagorri, J. A. Fernández, *Polym. Degrad. Stab.* **2000**, 69, 11.
- [25] N. Miskolczi, T. Juzsakova, J. Sója, *J. Energy Inst.* **2019**, 92, 118.
- [26] G. Elordi, M. Olazar, G. Lopez, P. Castaño, J. Bilbao, *Appl. Catal., B* **2011**, 102, 224.
- [27] S. D. Anuar Sharuddin, F. Abnisa, W. M. A. Wan Daud, M. K. Aroua, *Energy Convers. Manage.* **2016**, 115, 308.
- [28] K. Moorthy Rajendran, V. Chintala, A. Sharma, S. Pal, J. K. Pandey, P. Ghodke, *Mater. Today Commun.* **2020**, 24, 100982.
- [29] M. Boronat, A. Corma, *Catal. Lett.* **2015**, 145, 162.
- [30] J. F. Mastral, C. Berruero, M. Gea, J. Ceamanos, *Polym. Degrad. Stab.* **2006**, 91, 3330.
- [31] G. Lopez, M. Artetxe, M. Amutio, J. Bilbao, M. Olazar, *Renewable Sustainable Energy Rev.* **2017**, 73, 346.
- [32] M. S. Abbas-Abadi, M. N. Haghighi, H. Yeganeh, *Fuel Process. Technol.* **2013**, 109, 90.
- [33] M. S. Abbas-Abadi, M. N. Haghighi, H. Yeganeh, *J. Anal. Appl. Pyrolysis* **2012**, 95, 198.
- [34] V. Daligaux, R. Richard, M. H. Manero, *Catalysts* **2021**, 11, 770.
- [35] S. Martey, B. Addison, N. Wilson, B. Tan, J. Yu, J. R. Dorgan, M. J. Sobkowicz, *ChemSusChem* **2021**, 14, 4280.
- [36] A. Marcilla, M. Hernández, A. García, *J. Anal. Appl. Pyrolysis* **2007**, 79, 424.
- [37] I. Muhammad, G. Manos, *Process Saf. Environ. Prot.* **2021**, 146, 702.
- [38] V. P. S. Caldeira, A. G. D. Santos, D. S. Oliveira, R. B. Lima, L. D. Souza, S. B. C. Pergher, *J. Therm. Anal. Calorim.* **2017**, 130, 1939.
- [39] D. P. Serrano, J. Aguado, J. M. Escola, E. Garagorri, *J. Anal. Appl. Pyrolysis* **2001**, 58–59, 789.
- [40] D. P. Serrano, J. Aguado, J. M. Escola, E. Garagorri, *Appl. Catal., B* **2003**, 44, 95.
- [41] A. Marcilla, A. Gómez, F. Valdés, *J. Anal. Appl. Pyrolysis* **2007**, 79, 433.
- [42] X. Tian, Z. Zeng, Z. Liu, L. Dai, J. Xu, X. Yang, L. Yue, Y. Liu, R. Ruan, Y. Wang, *J. Clean. Prod.* **2022**, 358, 131989.
- [43] I. C. Neves, G. Botelho, A. V. Machado, P. Rebelo, *Eur. Polym. J.* **2006**, 42, 1541.
- [44] H. Wang, W. Xin, *Catal. Lett.* **2001**, 76, 225.
- [45] A. Aho, N. Kumar, K. Eränen, T. Salmi, M. Hupa, D. Y. Murzin, *Process Saf. Environ. Prot.* **2007**, 85, 473.
- [46] Y. Miyamoto, N. Katada, M. Niwa, *Microporous Mesoporous Mater.* **2000**, 40, 271.
- [47] J. Agullo, N. Kumar, D. Berenguer, D. Kubicka, A. Marcilla, A. Gómez, T. Salmi, D. Y. Murzin, *Kinet. Catal.* **2007**, 48, 535.
- [48] J. Aguado, D. P. Serrano, G. S. Miguel, J. M. Escola, J. M. Rodríguez, *J. Anal. Appl. Pyrolysis* **2007**, 78, 153.
- [49] P. Rex, V. Ganesan, V. Sivashankar, S. Tajudeen, *Int. J. Environ. Sci. Technol.* **2022**, 20, 8141.
- [50] G. Elordi, M. Olazar, G. Lopez, M. Amutio, M. Artetxe, R. Aguado, J. Bilbao, *J. Anal. Appl. Pyrolysis* **2009**, 85, 345.
- [51] Y. J. Lee, J. H. Kim, S. H. Kim, S. B. Hong, G. Seo, *Appl. Catal., B* **2008**, 83, 160.
- [52] S. T. Okonsky, J. V. J. Krishna, H. E. Toraman, *React. Chem. Eng.* **2022**, 7, 2175.
- [53] A. Marcilla, M. I. Beltrán, F. Hernández, R. Navarro, *Appl. Catal., A* **2004**, 278, 37.
- [54] L. Dai, N. Zhou, H. Li, Y. Wang, Y. Liu, K. Cobb, Y. Cheng, H. Lei, P. Chen, R. Ruan, *Sci. Total Environ.* **2021**, 771, 144995.
- [55] J. Wang, J. Jiang, X. Wang, S. Pang, Y. Sun, X. Meng, M. Li, R. Ruan, A. J. Ragauskas, *Fuel* **2020**, 278, 118322.
- [56] P. Gaurh, H. Pramanik, *Waste Manage.* **2018**, 77, 114.
- [57] M. Cocchi, D. De Angelis, L. Mazzeo, P. Nardozi, V. Piemonte, R. Tuffi, S. Vecchio Cipriotti, *Catalysts* **2020**, 10, 1113.
- [58] M. S. Renzini, L. C. Lerici, U. Sedran, L. B. Pierella, *J. Anal. Appl. Pyrolysis* **2011**, 92, 450.
- [59] S. Kumar, A. K. Panda, R. K. Singh, *Resour. Conserv. Recycl.* **2011**, 55, 893.

- [60] D. P. Serrano, J. Aguado, J. M. Escola, J. M. Rodríguez, *J. Anal. Appl. Pyrolysis* **2005**, 74, 353.
- [61] D. Fu, A. Lucini Paioni, C. Lian, O. van der Heijden, M. Baldus, B. M. Weckhuysen, *Angew. Chem., Int. Ed.* **2020**, 59, 20024.
- [62] Q. Zhang, K. Qiu, B. Li, T. Jiang, X. Zhang, L. Ma, T. Wang, *Fuel* **2011**, 90, 3468.
- [63] S. J. Han, S. K. Kim, A. Hwang, S. Kim, D. Y. Hong, G. Kwak, K. W. Jun, Y. T. Kim, *Appl. Catal., B* **2019**, 241, 305.
- [64] M. Rahman, A. Infantes-Molina, A. S. Hoffman, S. R. Bare, K. L. Emerson, S. J. Khatib, *Fuel* **2020**, 278, 118290.
- [65] Y. Zhang, S. Wu, X. Xu, H. Jiang, *Catal. Sci. Technol.* **2020**, 10, 835.
- [66] F. J. Sotomayor, K. A. Cychosz, M. Thommes, *Acc. Mater. Surf. Res* **2018**, 3, 34.
- [67] C. Zhang, S. Li, S. Bao, *Waste Biomass Valorization* **2019**, 10, 2825.
- [68] J. Aguado, D. P. Serrano, J. M. Escola, L. Briones, *Fuel* **2013**, 109, 679.
- [69] X. Hou, L. Zhao, Z. Diao, *Catal. Lett.* **2020**, 150, 2716.
- [70] Y. Fan, X. Bao, G. Shi, *Catal. Lett.* **2005**, 105, 67.
- [71] P. Castaño, G. Elordi, M. Olazar, A. T. Aguayo, B. Pawelec, J. Bilbao, *Appl. Catal., B* **2011**, 104, 91.
- [72] Y. Bi, X. Lei, G. Xu, H. Chen, J. Hu, *Catalysts* **2018**, 8, 82.
- [73] M. Heydariaraghi, S. Ghorbanian, A. Hallajisani, A. Salehpour, *J. Anal. Appl. Pyrolysis* **2016**, 121, 307.
- [74] Y. K. Park, J. S. Jung, J. Jae, S. B. Hong, A. Watanabe, Y. M. Kim, *Chem. Eng. J.* **2019**, 377, 119742.
- [75] N. Miskolczi, J. Sója, E. Tulok, *J. Anal. Appl. Pyrolysis* **2017**, 128, 1.
- [76] S. P. D. S. Ribeiro, R. C. Martins, G. M. Barbosa, M. A. D. F. Rocha, A. Landesmann, M. A. C. Nascimento, R. S. V. Nascimento, *J. Mater. Sci.* **2020**, 55, 619.